

Symmetry-mode-based classical and quantum mechanical formalism of lattice dynamics

Tsezar F. Seman¹, Jichan Moon² and K. H. Ahn^{1*}

¹*Department of Physics, New Jersey Institute of Technology, Newark, New Jersey 07102, USA*

²*Department of Physics, Konkuk University, Seoul, 143-701, South Korea*

We present classical and quantum mechanical descriptions of lattice dynamics, from the atomic to the continuum scale, using atomic scale symmetry modes and their constraint equations. This approach is demonstrated for a one-dimensional chain and a two-dimensional square lattice with a monatomic basis. For the classical description, we find that rigid modes, in addition to the distortional modes found before, are necessary to describe the kinetic energy. The long wavelength limit of the kinetic energy terms expressed in terms of atomic scale modes is shown to be consistent with the continuum theory, and the leading order corrections are obtained. For the quantum mechanical description, we find conjugate momenta for the atomic scale symmetry modes. In direct space, graphical rules for their commutation relations are obtained. Commutation relations in the reciprocal space are also calculated. As an example, phonon modes are analyzed in terms of symmetry modes. We emphasize that the approach based on atomic scale symmetry modes could be useful, for example, for the description of multiscale lattice dynamics and the dynamics near structural phase transition.

PACS numbers: 61.50.Ah, 63.20.D-, 63.22.-m, 62.20.-x

I. INTRODUCTION

The dynamics at nanometer length scale has been a focus of recent attention.¹ In particular, materials with competing ground states, such as high temperature superconducting cuprates and colossal magnetoresistive manganites,²⁻⁴ often show dynamic nanometer scale features, for example, stripes in cuprates^{5,6} and anisotropic correlations in manganites.^{7,8} Furthermore, recent advances in time-resolved x-ray technique have allowed experimenters to directly probe lattice dynamics in atomic scale.⁹ It is believed that understanding these nanoscale features and their dynamics is essential to explain macroscopic properties of these materials.

For the description of mesoscopic scale domain structures and their dynamics, phenomenological Ginzburg-Landau formalism has been very successful.^{10,11} One of the keys for such a success is the use of symmetry in the definition of variables, which makes the selection of free energy terms self-evident. Motivated by the success of the Ginzburg-Landau approach for the continuum, symmetry-based atomic scale description of lattice distortions has been recently proposed, and demonstrated for a two-dimensional square lattice.¹² In this approach, atomic scale symmetry modes are defined on a plaquette of atoms, and are used to express potential energy terms associated with lattice distortions. This method has been used to understand atomic scale structure of twin boundaries,¹² antiphase boundaries and their electronic textures,¹³ strain-induced metal-insulator phase coexistence in manganites,⁸ superconducting order parameter textures around structural defects,¹⁴ and the coupling between electronic nematic order parameter and structural domains in metamagnets near a quantum critical point.¹⁵ Thus far, this approach has been used for static lattices, or the relaxation of lattice distortions introduced through

the Euler method,¹⁰ which does not require kinetic energy terms. In the current paper, we present our study on how the approach based on atomic scale symmetry modes can be extended to describe lattice dynamics, within the scope of both classical and quantum mechanical formalism. In Section II, we discuss how to express kinetic energy term in symmetry modes, present our study within the formalism of classical mechanics and compare our result with the continuum results.¹¹ We formulate quantum mechanics in terms of atomic scale symmetry modes in Section III, with a summary given in Section IV. Appendix A presents a simple demonstration of symmetry-mode-based approach for lattice dynamics, that is, the phonon mode analysis in terms of symmetry modes.

II. CLASSICAL FORMALISM

A. One-dimensional lattice with a monatomic basis

Using a one-dimensional lattice with a monatomic basis shown in Fig. 1, we demonstrate the concept of the mode-based description of lattice dynamics. The dis-

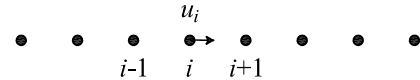


FIG. 1. One-dimensional lattice with a monatomic basis.

placements of atoms are represented by u_i , where i being an index for the site. To be specific, we assume that the interaction between the nearest neighbor atoms are described by a spring with a spring constant K while other potential energy terms are negligible, as represented by

the following Lagrangian,

$$L_{\text{chain}} = \sum_i \frac{1}{2} M \dot{u}_i^2 - \frac{1}{2} K (u_{i+1} - u_i)^2, \quad (1)$$

where M is the mass of the atom. We take a two-atom unit as a motif for this lattice, and define the symmetry modes, $e(i)$ and $t(i)$,

$$e(i) \equiv \frac{1}{\sqrt{2}} (u_{i+1} - u_i), \quad (2)$$

$$t(i) \equiv \frac{1}{\sqrt{2}} (u_{i+1} + u_i), \quad (3)$$

where a normalization factor is chosen according to the number of displacement variables in the definition. These modes are also shown in Fig. 2.



FIG. 2. Symmetry modes for the one-dimensional chain in Fig. 1.

The two variables, e and t , correspond to the distortion and rigid translation of the motif, respectively. Since the two modes are defined from one physically independent displacement variable at each site i , these modes are related through one constraint equation shown below in the reciprocal space and direct space, respectively.

$$f(k) \equiv (e^{ik} + 1)e(k) - (e^{ik} - 1)t(k) = 0, \quad (4)$$

$$e(i+1) + e(i) - t(i+1) + t(i) = 0. \quad (5)$$

In terms of these modes, the Lagrangian in Eq. (1) is expressed in the following way

$$L_{\text{chain}} = \sum_i \frac{1}{2} \left(\frac{M}{2} \right) [\dot{e}(i)^2 + \dot{t}(i)^2] - \frac{1}{2} (2K) e(i)^2. \quad (6)$$

The result shows that introduction of atomic scale rigid modes, such as t , which are not considered in Ref. 12, allows kinetic energy term being expressed in a quadratic form. To obtain equations of motion, we modify L_{chain} with a Lagrange multiplier $\lambda(k)$, as shown below.

$$\begin{aligned} \tilde{L}_{\text{chain}} = \sum_k \frac{1}{2} \left(\frac{M}{2} \right) & [\dot{e}(k)\dot{e}(-k) + \dot{t}(k)\dot{t}(-k)] \\ & - \frac{1}{2} (2K) e(k)e(-k) + \lambda(k)f(-k). \end{aligned} \quad (7)$$

The Lagrangian formalism of dynamics leads to the two equations of motion,

$$\frac{M}{2} \ddot{e}(k) + 2K e(k) - \lambda(k)(e^{-ik} + 1) = 0, \quad (8)$$

$$\frac{M}{2} \ddot{t}(k) + \lambda(k)(e^{-ik} - 1) = 0, \quad (9)$$

and a well-known dispersion relation for the one-dimensional chain,¹⁶

$$\omega = \sqrt{\frac{K}{M}} (1 - \cos k). \quad (10)$$

This result shows that the lattice dynamics can be studied within the framework of atomic scale symmetry modes and their constraint equations, without using the displacement variables explicitly.

Anharmonicity of one-dimensional chains is important to understand non-linear excitations, such as solitons, kink-solitons, intrinsically localized modes, and breathers.^{17,18} Atomic scale modes, e and t , found here can be used to incorporate such anharmonicity into the Hamiltonian, which, along with their constraint equations, would provide a formalism to study the dynamics of non-linear excitations in one-dimensional chains. In the next subsection, we demonstrate how the mode-based approach is applied to lattice dynamics for a two-dimensional square lattice with a monatomic basis.

B. Two-dimensional square lattice with a monatomic basis

Symmetry-based atomic scale description of lattice distortions for a two-dimensional square lattice with a monatomic basis, shown in Fig. 3, has been studied in Ref. 12, where dilatational e_1 , shear e_2 , and deviatoric e_3 modes, and short wavelength modes, s_x and s_y , are defined, as shown in Fig. 4. In terms of displacement variables u_i^x and u_i^y , and i_x and i_y representing site indices, these distortional symmetry modes are expressed

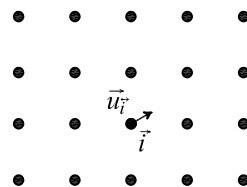


FIG. 3. Two-dimensional square lattice with a monatomic basis.

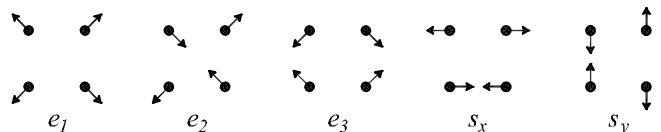


FIG. 4. Distortional symmetry modes of the motif for the two-dimensional square lattice with a monatomic basis in Fig. 3.

as follows.

$$e_1(\vec{i}) = \frac{1}{2\sqrt{2}} \left(-u_i^x - u_i^y + u_{i+10}^x - u_{i+10}^y - u_{i+01}^x + u_{i+01}^y + u_{i+11}^x + u_{i+11}^y \right), \quad (11)$$

$$e_2(\vec{i}) = \frac{1}{2\sqrt{2}} \left(-u_i^x - u_i^y - u_{i+10}^x + u_{i+10}^y + u_{i+01}^x - u_{i+01}^y + u_{i+11}^x + u_{i+11}^y \right), \quad (12)$$

$$e_3(\vec{i}) = \frac{1}{2\sqrt{2}} \left(-u_i^x + u_i^y + u_{i+10}^x + u_{i+10}^y - u_{i+01}^x - u_{i+01}^y + u_{i+11}^x - u_{i+11}^y \right), \quad (13)$$

$$s_x(\vec{i}) = \frac{1}{2} \left(u_i^x - u_{i+10}^x - u_{i+01}^x + u_{i+11}^x \right), \quad (14)$$

$$s_y(\vec{i}) = \frac{1}{2} \left(u_i^y - u_{i+10}^y - u_{i+01}^y + u_{i+11}^y \right). \quad (15)$$

Instead of s_x and s_y modes, the following s_+ and s_- modes can be also used.

$$s_+(\vec{i}) = \frac{1}{\sqrt{2}} [s_x(\vec{i}) + s_y(\vec{i})], \quad (16)$$

$$s_-(\vec{i}) = \frac{1}{\sqrt{2}} [s_x(\vec{i}) - s_y(\vec{i})]. \quad (17)$$

These five modes have been used to express various harmonic and anharmonic potential energy terms,^{8,12,13} but are not sufficient to represent kinetic energy terms in a simple quadratic form.

In current work, we show that additional modes associated with the rigid motion of the motif, similar to the mode t in the one-dimensional chain, allow a formalism entirely based on symmetry modes without resorting to displacement variables. Three rigid modes for the two-dimensional square lattice are shown in Fig. 5 and are defined as follows.

$$t_x(\vec{i}) = \frac{1}{2} \left(u_i^x + u_{i+10}^x + u_{i+01}^x + u_{i+11}^x \right), \quad (18)$$

$$t_y(\vec{i}) = \frac{1}{2} \left(u_i^y + u_{i+10}^y + u_{i+01}^y + u_{i+11}^y \right), \quad (19)$$

$$r(\vec{i}) = \frac{1}{2\sqrt{2}} \left(u_i^x - u_i^y + u_{i+10}^x + u_{i+10}^y - u_{i+01}^x - u_{i+01}^y - u_{i+11}^x + u_{i+11}^y \right). \quad (20)$$

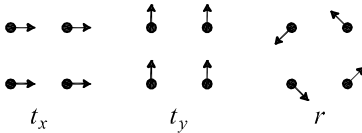


FIG. 5. Rigid symmetry modes of the motif for the two-dimensional square lattice with a monatomic basis in Fig. 3.

The first two modes, t_x and t_y , correspond to rigid translations of the motif along x and y direction, and the mode

r represents a rigid rotation of the motif. Following t_+ and t_- modes can be also used as alternatives to t_x and t_y .

$$t_+(\vec{i}) = \frac{1}{\sqrt{2}} [t_x(\vec{i}) + t_y(\vec{i})], \quad (21)$$

$$t_-(\vec{i}) = \frac{1}{\sqrt{2}} [t_x(\vec{i}) - t_y(\vec{i})]. \quad (22)$$

Straight-forward expansion shows that the kinetic energy of the lattice is expressed in terms of the eight symmetry modes in the following quadratic form, with M being the mass of the atom.

$$\begin{aligned} T_{\text{sq}} &= \sum_{\vec{i}} \frac{1}{2} M [(\dot{u}_{\vec{i}}^x)^2 + (\dot{u}_{\vec{i}}^y)^2] \\ &= \sum_{\vec{i}} \frac{1}{2} \left(\frac{M}{4} \right) [\dot{e}_1(\vec{i})^2 + \dot{e}_2(\vec{i})^2 + \dot{e}_3(\vec{i})^2 + \dot{s}_x(\vec{i})^2 \\ &\quad + \dot{s}_y(\vec{i})^2 + \dot{t}_x(\vec{i})^2 + \dot{t}_y(\vec{i})^2 + \dot{r}(\vec{i})^2]. \end{aligned} \quad (24)$$

As discussed in Ref. 12, constraint equations are found from the relations between symmetry modes and displacement variables in the reciprocal space. We first represent $(u_{\vec{k}}^x, u_{\vec{k}}^y)$ in terms of $(s_x(\vec{k}), s_y(\vec{k}))$ by inverting the linear relations between them, and replace in the expressions with other modes, which lead to six constraint equations.¹⁹

$$\begin{aligned} \sin \frac{k_x}{2} \cos \frac{k_y}{2} s_x(\vec{k}) + \cos \frac{k_x}{2} \sin \frac{k_y}{2} s_y(\vec{k}) - \\ - \sqrt{2} i \sin \frac{k_x}{2} \sin \frac{k_y}{2} e_1(\vec{k}) = 0, \end{aligned} \quad (25)$$

$$\begin{aligned} \cos \frac{k_x}{2} \sin \frac{k_y}{2} s_x(\vec{k}) + \sin \frac{k_x}{2} \cos \frac{k_y}{2} s_y(\vec{k}) - \\ - \sqrt{2} i \sin \frac{k_x}{2} \sin \frac{k_y}{2} e_2(\vec{k}) = 0, \end{aligned} \quad (26)$$

$$\begin{aligned} \sin \frac{k_x}{2} \cos \frac{k_y}{2} s_x(\vec{k}) - \cos \frac{k_x}{2} \sin \frac{k_y}{2} s_y(\vec{k}) - \\ - \sqrt{2} i \sin \frac{k_x}{2} \sin \frac{k_y}{2} e_3(\vec{k}) = 0, \end{aligned} \quad (27)$$

$$\begin{aligned} \cos \frac{k_x}{2} \sin \frac{k_y}{2} s_x(\vec{k}) - \sin \frac{k_x}{2} \cos \frac{k_y}{2} s_y(\vec{k}) + \\ + \sqrt{2} i \sin \frac{k_x}{2} \sin \frac{k_y}{2} r(\vec{k}) = 0, \end{aligned} \quad (28)$$

$$\cos \frac{k_x}{2} \cos \frac{k_y}{2} s_x(\vec{k}) + \sin \frac{k_x}{2} \sin \frac{k_y}{2} t_x(\vec{k}) = 0, \quad (29)$$

$$\cos \frac{k_x}{2} \cos \frac{k_y}{2} s_y(\vec{k}) + \sin \frac{k_x}{2} \sin \frac{k_y}{2} t_y(\vec{k}) = 0. \quad (30)$$

Modified Lagrangian for the square lattice is now

$$\tilde{L}_{\text{sq}} = T_{\text{sq}} - V + \sum_{n=1}^6 \sum_{\vec{k}} \lambda_n(\vec{k}) f_n(-\vec{k}), \quad (31)$$

where V is the potential energy, $\lambda_n(\vec{k})$ are Lagrange multipliers, and $f_n(\vec{k}) = 0$ are the six constraint equations, Eqs. (25) - (30). By solving the Lagrangian equations, we find dynamic properties of the lattice in terms of the symmetry modes. As with the Ginzburg-Landau approach being useful for the description of mesoscale dynamics, we expect that the approach based on atomic scale symmetry modes would be useful for the description of atomic scale dynamics, particularly, when anharmonicity plays an essential role.

C. Comparison with continuum description of lattice dynamics

We compare the atomic scale theory developed in the previous subsection with an existing continuum theory of lattice dynamics. Either by using the definitions, Eqs. (11) and (13), or by using the constraint equations, we express the kinetic energy for the square lattice, Eqs. (23) and (24), in terms of e_1 and e_3 ,

$$T_{\text{sq}} = \sum_{\vec{k}} \sum_{s=1,3} \sum_{s'=1,3} \frac{1}{2} M \gamma_{ss'}(\vec{k}) \dot{e}_s(\vec{k}) \dot{e}_{s'}(-\vec{k}), \quad (32)$$

where

$$\gamma_{11}(\vec{k}) = \gamma_{33}(\vec{k}) = \frac{1 - \cos k_x \cos k_y}{\sin^2 k_x \sin^2 k_y}, \quad (33)$$

$$\gamma_{13}(\vec{k}) = \gamma_{31}(\vec{k}) = \frac{\cos k_x - \cos k_y}{\sin^2 k_x \sin^2 k_y}. \quad (34)$$

To compare with a continuum theory, we take the long wavelength limit, and obtain the following leading order term for $\gamma_{ss'}$,

$$\gamma_{ss'}^{(0)}(\vec{k}) = \begin{pmatrix} \frac{k_x^2 + k_y^2}{2k_x^2 k_y^2} & \frac{k_y^2 - k_x^2}{2k_x^2 k_y^2} \\ \frac{k_y^2 - k_x^2}{2k_x^2 k_y^2} & \frac{k_x^2 + k_y^2}{2k_x^2 k_y^2} \end{pmatrix}. \quad (35)$$

This term is identical to Eq. (3.12a) in Ref. 11 (e_3 here corresponds to e_2 in Ref. 11), which Lookman *et al.* have used as continuum kinetic energy to study underdamped dynamics of strains in proper ferroelastic materials. The next order term to the above continuum limit is as follows.

$$\gamma_{ss'}^{(1)}(\vec{k}) = \begin{pmatrix} \frac{1}{12} + \frac{k_x^4 + k_y^4}{8k_x^2 k_y^2} & \frac{k_y^4 - k_x^4}{8k_x^2 k_y^2} \\ \frac{k_y^4 - k_x^4}{8k_x^2 k_y^2} & \frac{1}{12} + \frac{k_x^4 + k_y^4}{8k_x^2 k_y^2} \end{pmatrix}. \quad (36)$$

This term, or better Eqs. (33) and (34), can be used to study the dynamics of proper ferroelastic materials on the atomic scale. The following long wavelength limit of the atomic scale modes shows directly what they correspond

to in the continuum theory.

$$e_1(\vec{i}) = \frac{1}{\sqrt{2}} [\nabla_x u_i^x + \nabla_y u_i^y], \quad (37)$$

$$e_2(\vec{i}) = \frac{1}{\sqrt{2}} [\nabla_x u_i^y + \nabla_y u_i^x], \quad (38)$$

$$e_3(\vec{i}) = \frac{1}{\sqrt{2}} [\nabla_x u_i^x - \nabla_y u_i^y], \quad (39)$$

$$r(\vec{i}) = \frac{1}{\sqrt{2}} [\nabla_x u_i^y - \nabla_y u_i^x], \quad (40)$$

$$s_x(\vec{i}) = \frac{1}{2} \nabla_x \nabla_y u_i^x, \quad (41)$$

$$s_y(\vec{i}) = \frac{1}{2} \nabla_x \nabla_y u_i^y, \quad (42)$$

$$t_x(\vec{i}) = 2u_i^x, \quad (43)$$

$$t_y(\vec{i}) = 2u_i^y. \quad (44)$$

In $k \rightarrow 0$ limit, the correspondence of these modes to the displacements u are

$$\begin{aligned} t_x, t_y &\sim u, \\ e_1, e_2, e_3, r &\sim ku, \\ s_x, s_y &\sim k^2 u. \end{aligned} \quad (45)$$

The comparison shows that our approach is a natural extension of the continuum theory to the atomic scale, and is suitable for multiscale description of lattice dynamics.

III. QUANTUM MECHANICAL FORMALISM

A. One-dimensional lattice with a monatomic basis

It is necessary to consider quantum mechanical aspects of lattice dynamics for phenomena such as low temperature specific heat, electron-phonon interaction, and polarons. In this section, we extend the symmetry-based atomic scale description of lattice dynamics to the quantum mechanical formalism. Commutation relations between the coordinate operators and their conjugate momentum operators lie at the core of quantum mechanics, which we establish here for the symmetry modes.

First, we consider the one-dimensional chain studied in Section II.A. The conjugate momenta for the two modes, $P_e(i)$ and $P_t(i)$ are

$$P_e(i) = \frac{\partial L}{\partial \dot{e}(i)} = \frac{M}{2} \dot{e}(i) = \frac{1}{2\sqrt{2}} (p_{i+1} - p_i), \quad (46)$$

$$P_t(i) = \frac{\partial L}{\partial \dot{t}(i)} = \frac{M}{2} \dot{t}(i) = \frac{1}{2\sqrt{2}} (p_{i+1} + p_i), \quad (47)$$

where p_i represents the momentum of the atom at site i . From known commutation relations between momentum and displacement operators \hat{p}_i and \hat{u}_j , we find the following commutation relations between the operators for modes and their conjugate momenta with the same site

index i ,

$$[P_a(i), b(i)] = \frac{\hbar}{2i} \delta_{ab},$$

where $a, b \in \{e, t\}$. The $1/2$ factor is related to the number of atoms in each motif. Unlike displacement variables, the commutation relation between a mode at i and a conjugate momentum at $i+1$ or $i-1$ is not zero, since they share an atom, as shown below.

$$[P_t(i), t(i \pm 1)] = [P_e(i), t(i+1)] = [P_t(i), e(i-1)] = \frac{\hbar}{4i},$$

$$[P_e(i), e(i \pm 1)] = [P_t(i), e(i+1)] = [P_e(i), t(i-1)] = \frac{-\hbar}{4i}.$$

The commutation relations between the momentum and the mode, defined at sites further than the nearest neighbors, vanish.

The above relations are also established graphically. For example, $[P_e(i), t(i+1)]$ is found from the drawing in Fig. 6, where $P_e(i)$ and $t(i+1)$ are represented with arrows. We treat the arrows as unit vectors, and find the

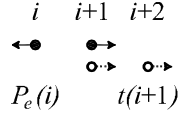


FIG. 6. Graph to find commutation relation, $[P_e(i), t(i+1)]$.

sum of scalar products of unit vectors defined at the same sites, which after being multiplied by $\hbar/(2^2i)$, lead to the commutation relation. From the graphical rule and the symmetry of the modes, the following commutations are obtained, where $a, b \in \{e, t\}$.

$$[P_a(i), b(j)] = [P_b(j), a(i)], \quad (48)$$

$$[P_e(i), t(j)] = -[P_t(i), e(j)]. \quad (49)$$

The commutation relations in reciprocal space are calculated from the relations,

$$[P_a(k), b(k')] = \delta_{k', -k} \sum_j [P_a(i=0), b(j)] e^{ikj}, \quad (50)$$

which are shown in Table I. The results found here are applicable, for example, for the study of quantum mechanical dynamics of non-linear excitations mentioned in Section II.A.

B. Two-dimensional square lattice with a monatomic basis

Quantum mechanical nature of lattice is also important for two or three-dimensional lattices, for example, near the structural phase transitions. In this subsection,

	$\frac{i}{\hbar} P_e(k)$	$\frac{i}{\hbar} P_t(k)$
$e(-k)$	$\frac{1}{2}(1 - \cos k)$	$-\frac{i}{2} \sin k$
$t(-k)$	$\frac{i}{2} \sin k$	$\frac{1}{2}(1 + \cos k)$

TABLE I. Commutation relation, $[\frac{i}{\hbar} P_a(k), b(-k)]$, between symmetry modes and their conjugate momenta for the one-dimensional chain in reciprocal space.

we find quantum mechanical commutation relations for the symmetry modes and their conjugate momenta for the square lattice studied in Section II.B.

Conjugate momenta for the atomic scale symmetry modes are as follows.

$$P_{e_1}(\vec{i}) = \frac{M}{4} \dot{e}_1(\vec{i}) = \frac{1}{8\sqrt{2}} \left(-p_i^x - p_i^y + p_{i+10}^x - p_{i+10}^y - p_{i+01}^x + p_{i+01}^y + p_{i+11}^x + p_{i+11}^y \right),$$

$$P_{e_2}(\vec{i}) = \frac{M}{4} \dot{e}_2(\vec{i}) = \frac{1}{8\sqrt{2}} \left(-p_i^x - p_i^y - p_{i+10}^x + p_{i+10}^y + p_{i+01}^x - p_{i+01}^y + p_{i+11}^x + p_{i+11}^y \right),$$

$$P_{e_3}(\vec{i}) = \frac{M}{4} \dot{e}_3(\vec{i}) = \frac{1}{8\sqrt{2}} \left(-p_i^x + p_i^y + p_{i+10}^x + p_{i+10}^y - p_{i+01}^x - p_{i+01}^y + p_{i+11}^x - p_{i+11}^y \right),$$

$$P_r(\vec{i}) = \frac{M}{4} \dot{r}(\vec{i}) = \frac{1}{8\sqrt{2}} \left(p_i^x - p_i^y + p_{i+10}^x + p_{i+10}^y - p_{i+01}^x - p_{i+01}^y - p_{i+11}^x + p_{i+11}^y \right),$$

$$P_{s_x}(\vec{i}) = \frac{M}{4} \dot{s}_x(\vec{i}) = \frac{1}{8} \left(p_i^x - p_{i+10}^x - p_{i+01}^x + p_{i+11}^x \right),$$

$$P_{s_y}(\vec{i}) = \frac{M}{4} \dot{s}_y(\vec{i}) = \frac{1}{8} \left(p_i^y - p_{i+10}^y - p_{i+01}^y + p_{i+11}^y \right),$$

$$P_{t_x}(\vec{i}) = \frac{M}{4} \dot{t}_x(\vec{i}) = \frac{1}{8} \left(p_i^x + p_{i+10}^x + p_{i+01}^x + p_{i+11}^x \right),$$

$$P_{t_y}(\vec{i}) = \frac{M}{4} \dot{t}_y(\vec{i}) = \frac{1}{8} \left(p_i^y + p_{i+10}^y + p_{i+01}^y + p_{i+11}^y \right).$$

From the fundamental commutation relations for displacement operators and momentum operators,

$$[p_i^x, u_j^x] = [p_i^y, u_j^y] = \frac{\hbar}{i} \delta_{\vec{i}, \vec{j}},$$

$$[p_i^x, u_j^y] = [p_i^y, u_j^x] = 0,$$

the commutation relations between modes and their conjugate momenta are calculated in a straight forward way.

However, it is more convenient to use the graphical method, explained for the one-dimensional chain in the previous subsection. The above fundamental commutation relations for $\vec{i} = \vec{j}$ have the form of

$$\hat{x} \cdot \hat{x} = \hat{y} \cdot \hat{y} = 1,$$

$$\hat{x} \cdot \hat{y} = \hat{y} \cdot \hat{x} = 0,$$

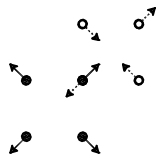


FIG. 7. Graph to find commutation relation, $[P_{e_1}(\vec{i}), e_2(\vec{i} + 11)]$.

except for the factor \hbar/i , where \hat{x} and \hat{y} represent unit vectors, not operators. Therefore, the commutation relation $[P_a(\vec{i}), b(\vec{j})]$, where a and b represent the eight atomic scale modes, is found from the drawings of a and b modes on the square lattice. The sum of the scalar products of the unit vectors at the sites shared by the two modes, multiplied by $\hbar/(4^2i)$, gives the commutation of the two operators. (The multiplication factor after \hbar/i is associated with the number of atoms in the motif for the lattice with a monatomic basis, that is 4 for the square lattice and 2 for the chain.) For example, $[P_{e_1}(\vec{i}), e_2(\vec{i} + 11)]$ is found from Fig. 7, as follows

$$[P_{e_1}(\vec{i}), e_2(\vec{i} + 11)] = \frac{\hbar}{4^2i}(-1). \quad (51)$$

Presented graphical method is also useful to find the following symmetry-related properties of the commutation relations, where a and b represent any of the eight modes, and *even* and *odd* represent the modes with even symmetry under point reflection, namely, e_1, e_2, e_3, r , and the modes with odd symmetry, namely, s_x, s_y, t_x, t_y , respectively.

$$\begin{aligned} [P_a(\vec{i}), b(\vec{i})] &= \frac{1}{4} \frac{\hbar}{i} \delta_{ab}, \\ [P_a(\vec{i}), b(\vec{j})] &= [P_b(\vec{j}), a(\vec{i})], \\ [P_{\text{even}}(\vec{i}), \text{even}'(\vec{j})] &= [P_{\text{even}'(\vec{i})}, \text{even}(\vec{j})], \\ [P_{\text{even}}(\vec{i}), \text{odd}(\vec{j})] &= -[P_{\text{odd}}(\vec{i}), \text{even}(\vec{j})], \\ [P_{\text{odd}}(\vec{i}), \text{odd}'(\vec{j})] &= [P_{\text{odd}'(\vec{i})}, \text{odd}(\vec{j})]. \end{aligned}$$

The commutation relations in reciprocal space are found from the relation

$$[P_a(\vec{k}), b(\vec{k}')] = \delta_{\vec{k}, -\vec{k}'} \sum_{\vec{j}} [P_a(\vec{i} = 0), b(\vec{j})] e^{i\vec{k} \cdot \vec{j}}, \quad (52)$$

which are provided in Table II.

IV. SUMMARY

In this article, we have presented mode-based atomic scale description of lattice dynamics. It is found that not only the potential energy but also the kinetic energy is described in terms of the atomic scale modes, for which the inclusion of the rigid modes is essential. This approach

has been demonstrated for the one-dimensional chain and the two-dimensional square lattice with a monatomic basis. The comparison with a continuum model has shown that our approach is suitable for multiscale description of lattice dynamics. The approach has been extended to quantum mechanics, and the commutation relations have been obtained. We expect that this method would be useful in describing atomic scale lattice dynamics in systems with strong anharmonicity and complex energy landscape, which can be compared with the results from experiments, such as, time-resolved x-ray diffraction.

Appendix A: Example of the application of symmetry modes for lattice dynamics - Phonon mode analysis

As a simple demonstration for the application of symmetry modes, we analyze phonon modes in terms of atomic scale symmetry modes for the square lattice with a harmonic potential shown below.¹²

$$\begin{aligned} V_{\text{sq}} &= \sum_{\vec{i}} \frac{1}{2} A_1 e_1(\vec{i})^2 + \frac{1}{2} A_2 e_2(\vec{i})^2 + \frac{1}{2} A_3 e_3(\vec{i})^2 \\ &+ \frac{1}{2} B [s_x(\vec{i})^2 + s_y(\vec{i})^2]. \end{aligned} \quad (A1)$$

The phonon dispersion relation for this potential energy was presented in Ref. 12. Furthermore, the phonon mode at $\vec{k} = (\pi, \pi)$, both in the upper and the lower branch, was shown entirely composed of short wave length modes, s_x and s_y , due to the constraints. In general, at other \vec{k} points, the contribution of different symmetry modes to the phonon mode depends not only on the constraint equations, but also on the values of the elastic moduli in the energy expression. In this Appendix, we present our current study on such general expressions which describes how different symmetry modes contribute to phonon modes for the entire first Brillouin zone for the potential V_{sq} shown above.

The equation of motion using conventional displacement-based approach leads the expression for the normal mode at \vec{k} , $[u_x^\pm(\vec{k}), u_y^\pm(\vec{k})]$, where \pm represent the upper and lower branch, except for an overall factor. By using the \vec{k} -space relation between symmetry modes and displacements, which is obtained from Eqs. (11)-(20), we get the expression of $[e_1^\pm(\vec{k}), e_2^\pm(\vec{k}), e_3^\pm(\vec{k}), r^\pm(\vec{k}), s_x^\pm(\vec{k}), s_y^\pm(\vec{k}), t_x^\pm(\vec{k}), t_y^\pm(\vec{k})]$ for the phonon modes at \vec{k} , where \pm again represents the upper and the lower branches.²⁰ The results are shown in Table III, where $\beta_1 = 1 - \cos k_x \cos k_y$, $\beta_2 = -\sin k_x \sin k_y$, $\beta_3 = \cos k_x - \cos k_y$, $\beta_4 = (1 - \cos k_x)(1 - \cos k_y)$, $\beta_5 = (1 + \cos k_x)(1 + \cos k_y)$, and $a = (A_1 - A_2 + A_3)/(A_1 + A_2 - A_3)$. In this result, the overall factor of the normal mode is determined by the normalization condition $|u_x^\pm(\vec{k})|^2 + |u_y^\pm(\vec{k})|^2 = 4$,

	$\frac{i}{\hbar}P_{e1}(\vec{k})$	$\frac{i}{\hbar}P_{e2}(\vec{k})$	$\frac{i}{\hbar}P_{e3}(\vec{k})$	$\frac{i}{\hbar}P_r(\vec{k})$	$\frac{i}{\hbar}P_{sx}(\vec{k})$	$\frac{i}{\hbar}P_{sy}(\vec{k})$	$\frac{i}{\hbar}P_{tx}(\vec{k})$	$\frac{i}{\hbar}P_{ty}(\vec{k})$
$e_1(-\vec{k})$	$\frac{1-C_{kx}C_{ky}}{4}$	$\frac{S_{kx}S_{ky}}{4}$	$\frac{-C_{kx}+C_{ky}}{4}$	0	$\frac{i(1-C_{kx})S_{ky}}{4\sqrt{2}}$	$\frac{i(1-C_{ky})S_{kx}}{4\sqrt{2}}$	$\frac{i(1+C_{ky})S_{kx}}{-4\sqrt{2}}$	$\frac{i(1+C_{kx})S_{ky}}{-4\sqrt{2}}$
$e_2(-\vec{k})$	$\frac{S_{kx}S_{ky}}{4}$	$\frac{1-C_{kx}C_{ky}}{4}$	0	$\frac{-C_{kx}+C_{ky}}{4}$	$\frac{i(1-C_{ky})S_{kx}}{4\sqrt{2}}$	$\frac{i(1-C_{kx})S_{ky}}{4\sqrt{2}}$	$\frac{i(1+C_{kx})S_{ky}}{-4\sqrt{2}}$	$\frac{i(1+C_{ky})S_{kx}}{-4\sqrt{2}}$
$e_3(-\vec{k})$	$\frac{-C_{kx}+C_{ky}}{4}$	0	$\frac{1-C_{kx}C_{ky}}{4}$	$\frac{-S_{kx}S_{ky}}{4}$	$\frac{i(1-C_{kx})S_{ky}}{4\sqrt{2}}$	$\frac{i(1-C_{ky})S_{kx}}{-4\sqrt{2}}$	$\frac{i(1+C_{ky})S_{kx}}{-4\sqrt{2}}$	$\frac{i(1+C_{kx})S_{ky}}{4\sqrt{2}}$
$r(-\vec{k})$	0	$\frac{-C_{kx}+C_{ky}}{4}$	$\frac{-S_{kx}S_{ky}}{4}$	$\frac{1-C_{kx}C_{ky}}{4}$	$\frac{i(1-C_{ky})S_{kx}}{-4\sqrt{2}}$	$\frac{i(1-C_{kx})S_{ky}}{4\sqrt{2}}$	$\frac{i(1+C_{kx})S_{ky}}{4\sqrt{2}}$	$\frac{i(1+C_{ky})S_{kx}}{-4\sqrt{2}}$
$s_x(-\vec{k})$	$\frac{i(1-C_{kx})S_{ky}}{-4\sqrt{2}}$	$\frac{i(1-C_{ky})S_{kx}}{-4\sqrt{2}}$	$\frac{i(1-C_{kx})S_{ky}}{-4\sqrt{2}}$	$\frac{i(1-C_{ky})S_{kx}}{4\sqrt{2}}$	$\frac{(1-C_{kx})(1-C_{ky})}{4}$	0	$\frac{-S_{kx}S_{ky}}{4}$	0
$s_y(-\vec{k})$	$\frac{i(1-C_{ky})S_{kx}}{-4\sqrt{2}}$	$\frac{i(1-C_{kx})S_{ky}}{-4\sqrt{2}}$	$\frac{i(1-C_{ky})S_{kx}}{4\sqrt{2}}$	$\frac{i(1-C_{kx})S_{ky}}{-4\sqrt{2}}$	0	$\frac{(1-C_{kx})(1-C_{ky})}{4}$	0	$\frac{-S_{kx}S_{ky}}{4}$
$t_x(-\vec{k})$	$\frac{i(1+C_{ky})S_{kx}}{4\sqrt{2}}$	$\frac{i(1+C_{kx})S_{ky}}{4\sqrt{2}}$	$\frac{i(1+C_{ky})S_{kx}}{4\sqrt{2}}$	$\frac{i(1+C_{kx})S_{ky}}{-4\sqrt{2}}$	$\frac{-S_{kx}S_{ky}}{4}$	0	$\frac{(1+C_{kx})(1+C_{ky})}{4}$	0
$t_y(-\vec{k})$	$\frac{i(1+C_{kx})S_{ky}}{4\sqrt{2}}$	$\frac{i(1+C_{ky})S_{kx}}{4\sqrt{2}}$	$\frac{i(1+C_{kx})S_{ky}}{-4\sqrt{2}}$	$\frac{i(1+C_{ky})S_{kx}}{4\sqrt{2}}$	0	$\frac{-S_{kx}S_{ky}}{4}$	0	$\frac{(1+C_{kx})(1+C_{ky})}{4}$

TABLE II. Commutation relation, $[\frac{i}{\hbar}P_a(\vec{k}), b(-\vec{k})]$, between symmetry modes and their conjugate momenta for the two-dimensional square lattice in reciprocal space. C_{kx} , C_{ky} , S_{kx} , and S_{ky} represent $\cos k_x$, $\cos k_y$, $\sin k_x$, and $\sin k_y$, respectively.

that is, $|e_1^\pm(\vec{k})|^2 + |e_2^\pm(\vec{k})|^2 + |e_3^\pm(\vec{k})|^2 + |r^\pm(\vec{k})|^2 + |s_x^\pm(\vec{k})|^2 + |s_y^\pm(\vec{k})|^2 + |t_x^\pm(\vec{k})|^2 + |t_y^\pm(\vec{k})|^2 = 1$. To be specific, we show these expressions for a special case of $a = 1$, which corresponds to $A_2 = A_3$, in the last column of Table III and plot them within the first Brillouin

zone of the square lattice in Fig. 8. The results show the contributions of different symmetry modes to the upper and the lower branch phonon modes within the first Brillouin zone. Some of the features are discussed in the figure caption and Footnote 21.

* kenahn@njit.edu

¹ M. Rini, R. Tobey, N. Dean, J. Itatani, Y. Tomioka, Y. Tokura, R. W. Schoenlein, and A. Cavalleri, Nature (London) **449**, 72 (2007).

² M. B. Salamon and M. Jaime, Rev. Mod. Phys. **73**, 583 (2001).

³ A. J. Millis, Nature (London) **392**, 147 (1998).

⁴ S. Jin, T. H. Tiefel, M. McCormack, R. A. Fastnacht, R. Ramesh, and L. H. Chen, Science **264**, 413 (1994).

⁵ J. M. Tranquada, B. J. Sternlieb, J. D. Axe, Y. Nakamura, and S. Uchida, Nature (London) **375**, 561 (1995).

⁶ S. A. Kivelson, I. P. Bindloss, E. Fradkin, V. Oganesyan, J. M. Tranquada, A. Kapitulnik, and C. Howald, Rev. Mod. Phys. **75**, 1201 (2003).

⁷ V. Kiryukhin, New J. Phys. **6** 155 (2004).

⁸ K. H. Ahn, T. Lookman and A. R. Bishop, Nature (London) **428**, 401 (2004).

⁹ See, e.g., K. J. Gaffney and H. N. Chapman, Science **316**, 1444 (2005), and references therein.

¹⁰ S.R. Shenoy, T. Lookman, A. Saxena, and A. R. Bishop, Phys. Rev. B **60**, R12 537 (1999).

¹¹ T. Lookman, S. R. Shenoy, K. Ø. Rasmussen, A. Saxena, and A. R. Bishop, Phys. Rev. B **67**, 024114 (2003).

¹² K. H. Ahn, T. Lookman, A. Saxena, and A. R. Bishop, Phys. Rev. B **68**, 092101 (2003).

¹³ K. H. Ahn, T. Lookman, A. Saxena and A. R. Bishop, Phys. Rev. B **71**, 212102 (2005).

¹⁴ J.-X. Zhu, K. H. Ahn, Z. Nussinov, T. Lookman, A. V. Balatsky and A. R. Bishop, Phys. Rev. Lett. **91**, 057004 (2003).

¹⁵ H. Doh, Y. B. Kim, and K. H. Ahn, Phys. Rev. Lett. **98**, 126407 (2007).

¹⁶ C. Kittel, *Introduction to Solid State Physics*, 8th ed. (John Wiley and Sons, Inc., Singapore, 1986).

¹⁷ D. Chen, S. Aubry, and G. P. Tsironis, Phys. Rev. Lett. **77**, 4776 (1996).

¹⁸ Y. A. Kosevich, L. I. Manevitch, and A. V. Savin, Phys. Rev. E **77**, 046603 (2008).

Mode	General expression upper/lower branch	Special case: $a = 1$	
		upper branch	lower branch
$ e_1(\vec{k}) ^2$	$\frac{1}{8} \left(\beta_1 \pm \frac{\beta_2^2 + a\beta_3^2}{\sqrt{\beta_2^2 + a^2\beta_3^2}} \right)$	$\frac{\beta_1}{4}$	0
$ e_2(\vec{k}) ^2$	$\frac{1}{8} \left(\beta_1 \pm \frac{\beta_2^2 - a\beta_3^2}{\sqrt{\beta_2^2 + a^2\beta_3^2}} \right)$	$\frac{\beta_2^2}{4\beta_1}$	$\frac{\beta_3^2}{4\beta_1}$
$ e_3(\vec{k}) ^2$	$\frac{1}{8} \left(\beta_1 \mp \frac{\beta_2^2 - a\beta_3^2}{\sqrt{\beta_2^2 + a^2\beta_3^2}} \right)$	$\frac{\beta_3^2}{4\beta_1}$	$\frac{\beta_2^2}{4\beta_1}$
$ r(\vec{k}) ^2$	$\frac{1}{8} \left(\beta_1 \mp \frac{\beta_2^2 + a\beta_3^2}{\sqrt{\beta_2^2 + a^2\beta_3^2}} \right)$	0	$\frac{\beta_1}{4}$
$ s_x(\vec{k}) ^2$	$\frac{\beta_4}{8} \left(1 \mp \frac{a\beta_3}{\sqrt{\beta_2^2 + a^2\beta_3^2}} \right)$	$\frac{\beta_4}{8\beta_1} (\beta_1 - \beta_3)$	$\frac{\beta_4}{8\beta_1} (\beta_1 + \beta_3)$
$ s_y(\vec{k}) ^2$	$\frac{\beta_4}{8} \left(1 \pm \frac{a\beta_3}{\sqrt{\beta_2^2 + a^2\beta_3^2}} \right)$	$\frac{\beta_4}{8\beta_1} (\beta_1 + \beta_3)$	$\frac{\beta_4}{8\beta_1} (\beta_1 - \beta_3)$
$ t_x(\vec{k}) ^2$	$\frac{\beta_5}{8} \left(1 \mp \frac{a\beta_3}{\sqrt{\beta_2^2 + a^2\beta_3^2}} \right)$	$\frac{\beta_5}{8\beta_1} (\beta_1 - \beta_3)$	$\frac{\beta_5}{8\beta_1} (\beta_1 + \beta_3)$
$ t_y(\vec{k}) ^2$	$\frac{\beta_5}{8} \left(1 \pm \frac{a\beta_3}{\sqrt{\beta_2^2 + a^2\beta_3^2}} \right)$	$\frac{\beta_5}{8\beta_1} (\beta_1 + \beta_3)$	$\frac{\beta_5}{8\beta_1} (\beta_1 - \beta_3)$
$ s_+(\vec{k}) ^2$	$\frac{\beta_4}{8} \left(1 \mp \frac{\beta_2}{\sqrt{\beta_2^2 + a^2\beta_3^2}} \right)$	$\frac{\beta_4}{8\beta_1} (\beta_1 - \beta_2)$	$\frac{\beta_4}{8\beta_1} (\beta_1 + \beta_2)$
$ s_-(\vec{k}) ^2$	$\frac{\beta_4}{8} \left(1 \pm \frac{\beta_2}{\sqrt{\beta_2^2 + a^2\beta_3^2}} \right)$	$\frac{\beta_4}{8\beta_1} (\beta_1 + \beta_2)$	$\frac{\beta_4}{8\beta_1} (\beta_1 - \beta_2)$
$ t_+(\vec{k}) ^2$	$\frac{\beta_5}{8} \left(1 \mp \frac{\beta_2}{\sqrt{\beta_2^2 + a^2\beta_3^2}} \right)$	$\frac{\beta_5}{8\beta_1} (\beta_1 - \beta_2)$	$\frac{\beta_5}{8\beta_1} (\beta_1 + \beta_2)$
$ t_-(\vec{k}) ^2$	$\frac{\beta_5}{8} \left(1 \pm \frac{\beta_2}{\sqrt{\beta_2^2 + a^2\beta_3^2}} \right)$	$\frac{\beta_5}{8\beta_1} (\beta_1 + \beta_2)$	$\frac{\beta_5}{8\beta_1} (\beta_1 - \beta_2)$

TABLE III. Normalized symmetry-mode squared amplitude for phonons within the first Brillouin zone of the square lattice. For \pm and \mp , the upper sign corresponds to the upper branch, and the lower sign the lower branch. $\beta_1 = 1 - \cos k_x \cos k_y$, $\beta_2 = -\sin k_x \sin k_y$, $\beta_3 = \cos k_x - \cos k_y$, $\beta_4 = (1 - \cos k_x)(1 - \cos k_y)$, $\beta_5 = (1 + \cos k_x)(1 + \cos k_y)$, and $a = (A_1 - A_2 + A_3)/(A_1 + A_2 - A_3)$. Special case of $a = 1$ corresponds to the case of $A_2 = A_3$.

¹⁹ We note that inverting the relation between $(s_x(\vec{k}), s_y(\vec{k}))$ and (u_k^x, u_k^y) is not possible for certain wave vectors, for example, wave vectors with $k_x=0$ or $k_y=0$. In those cases, new constraint equations should be found from the definition of the modes.

²⁰ This can be also done without explicit use of displacement variables, as suggested by Eq. (31) and done for the 1-D chain.

²¹ If the two shape-changing modes, e_2 and e_3 , have identical moduli, the lattice sustains isotropic phonon dispersion

in the long wavelength limit, in which the lattice behaves like an isotropic continuous medium. Such medium would support longitudinal phonon modes in the upper branch and transverse phonon modes in the lower branch: the former rotationless and the latter locally area-preserving. In finite wavelength limit case, the dispersion relation of phonon modes become anisotropic, reflecting only 90° rotational symmetry of the square lattice, but the absence of rotational and area changing mode for the upper and the lower branch phonons, respectively, still holds.

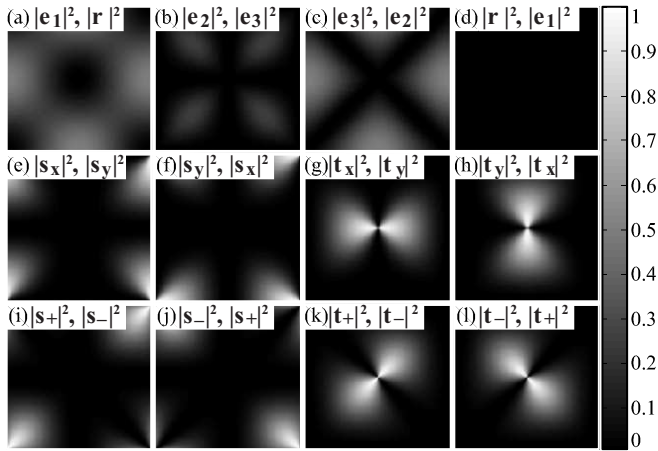


FIG. 8. Normalized symmetry-mode squared amplitude for phonons within the first Brillouin zone of the square lattice for $A_2 = A_3$, that is, $a = 1$, where $a = (A_1 - A_2 + A_3)/(A_1 + A_2 - A_3)$. The center of each square corresponds to $\vec{k} = (0, 0)$ and the four corners $\vec{k} = (\pm\pi, \pm\pi)$. Different modes in the upper branch and the lower branch have the same amplitude. The first and the second label for each panel indicate the mode for upper branch and lower branch, respectively. Therefore, for the upper branch, the twelve panels correspond to (a) $|e_1|^2$, (b) $|e_2|^2$, (c) $|e_3|^2$, (d) $|r|^2$, (e) $|s_x|^2$, (f) $|s_y|^2$, (g) $|t_x|^2$, (h) $|t_y|^2$, (i) $|s_+|^2$, (j) $|s_-|^2$, (k) $|t_+|^2$, and (l) $|t_-|^2$. For the lower branch, they correspond to (a) $|r|^2$, (b) $|e_3|^2$, (c) $|e_2|^2$, (d) $|e_1|^2$, (e) $|s_y|^2$, (f) $|s_x|^2$, (g) $|t_y|^2$, (h) $|t_x|^2$, (i) $|s_-|^2$, (j) $|s_+|^2$, (k) $|t_-|^2$, and (l) $|t_+|^2$. Panel (d) shows that the upper and lower branches of phonon modes remain locally rotationless and area-preserving, respectively, in this particular case of $A_2 = A_3$. This feature can be understood easily in the long wavelength limit from the fact that the sound velocity is isotropic for $A_2 = A_3$. See Footnote (21) for details. Such isotropic sound velocity for crystals can be useful for device applications.